

**Direct Measurement of the Structural Change Associated with Amorphous
Solidification using Elastic Scattering of Coherent Radiation**

Charlotte F. Petersen^{1,2} and Peter Harrowell^{1,*}

¹*School of Chemistry, University of Sydney, Sydney, New South Wales 2006 Australia*

²*School of Chemistry, University of Melbourne, Melbourne, Victoria 3010 Australia*

* Corresponding author: peter.harrowell@sydney.edu.au

Author contributions. Conceptualization - PH; Methodology – CFP + PH; Calculations - CFP; Writing – CFP + PH

Author Contact Information. charlotte.petersen@unimelb.edu.au &
peter.harrowell@sydney.edu.au

Abstract

In this paper we demonstrate that the weak temperature dependence of the structure factor of supercooled liquids, a defining feature of the glass transition, is a consequence of the averaging of the scattering intensity either due to the use of an incoherent radiation source or explicit angular averaging. We show that the speckle scattering at individual wavevectors, calculated from a simulated glass former, exhibits a sufficiently large temperature dependence to represent a structural order parameter capable of distinguishing liquid from glass. We also extract from the speckle intensities a quantity proportional to the variance of the local restraint, i.e. a direct experimental measure of the amplitude of structural heterogeneity.

1. Introduction

In a glass transition a fluid transforms into an amorphous solid when supercooled with little significant change in the scattering structure factor [1]. The conventional response to the challenge of describing the passage from fluid to solid in the absence of structural change is to eschew a microscopic description entirely and, instead, use the shear viscosity to measure solidification. This dynamic definition of solidification is awkward in that it is unsuitable for the characterization of the low temperature solid whose properties, including rigidity, arises from structural, rather than dynamic, origins. In this paper we address the possibility of experimentally measuring structural change directly associated with amorphous solidification. We establish, using simulations, that the amorphous Deby-Waller factor can be obtained from the static speckle scattering and that it can vary dramatically with temperature – from one at low temperatures to zero on heating, i.e. an experimentally measurable change in structure that is directly associated with amorphous solidification. We shall present a new analysis of scattering data that allows for direct experimental measurement of both atomic restraint and its heterogeneity.

Recently [2-4], we introduced a computational measure of the capacity of a configuration to restrain the motion of individual particles - exactly the type of structural order parameter needed to characterize amorphous solidification – and demonstrated that this

description provided interesting insights into liquid fragility, the influence of finite size and concentration of pinning sites [2-4] and the loss of restraint at the glass surface associated with observed enhanced kinetics [5]. These results suggest that a structural description of the transformation of a liquid into an amorphous solid can provide tractable and non-trivial insight into the phenomena associated with glass formation without the need to consider the viscosity or any other dynamic coefficient. Since the relationship between structure and dynamics will be complex and nonlinear we should treat a structural transformation as being distinct from a kinetic one. To keep this distinction clear we shall refer to the structural transformation as *amorphous solidification* and leave the term *glass transition* to refer to the dynamic transformation. The term ‘amorphous solidification’ does not imply any underlying thermodynamic singularity. All we assume in the following analysis is that the low temperature state is mechanically stable.

This paper is organized as follows. In the following Section we provide a brief background on Debye-Waller factor in crystal and amorphous solids. In Section 3 we consider the temperature dependence of static scattering intensities from an incoherent source and in Section 4 we present results from the analysis of the temperature dependence of speckle scattering from a coherent radiation source.

2. Debye-Waller factors in Crystals and Amorphous Solids

The Debye-Waller factor was originally formulated to account for the reduction of the elastic scattering intensity at Bragg peaks of a crystal due to the disorder introduced by thermally excited vibrations [6]. This reduction is conventionally expressed as

$$\frac{I(\vec{q}, T)}{I(\vec{q}, 0)} = \exp(-2W(\vec{q}, T)) \quad (1)$$

where the Debye-Waller (DW) factor, D_w , is

$$D_w(\vec{q}, T) = \exp(-2W(\vec{q}, T)) \quad (2)$$

If we assume that the fluctuations in atomic positions are small enough to be characterized as harmonic, then we can write [7]

$$W(\vec{q}, T) \approx \frac{1}{2} \left\langle (\vec{q} \cdot \vec{u}_i)^2 \right\rangle_{eq} \quad (3)$$

where \vec{u}_i is the displacement of atom i from its equilibrium position and the average $\langle \dots \rangle_{eq}$ is the equilibrium average over the harmonic Hamiltonian and the atoms in the system. In the context of X-ray crystallography, the DW factors are, unequivocally, structural measures, complimentary to the atomic positions. They or the associated mean squared displacement of atoms are standard outputs of structural determinations by X-ray diffraction [8]. Nonlinear least square fitting of the structure factors, such as the Rietveld method [9], treat both the mean atomic positions and the mean squared amplitudes atomic displacements as adjustable parameters.

Turning to amorphous materials, the Debye-Waller factor has been obtained from experiments that explicitly include inelastic processes. Buchenau and coworkers [10,11] have defined the DW factor for an amorphous material in terms of the inelastic neutron scattering spectrum $S(\vec{q}, \omega, T)$ as follows

$$D_w(q, T) = \frac{S_{el}(q, \Delta\omega, T)}{S(q, T)} \quad (4)$$

where $S_{el}(q, \Delta\omega) = \int_{-\Delta\omega}^{\Delta\omega} d\omega S(q, \omega)$ is the elastic component (defined by the frequency cut-

offs $\Delta\omega$ associated with the width of the elastic peak) and the structure factor $S(\vec{q}, T)$ is

$S(\vec{q}, T) = \int_{-\infty}^{\infty} d\omega S(\vec{q}, \omega, T)$. The DW factor, as defined in Eq. 4, is simply the elastic

fraction of the total scattering. An alternative definition of the amorphous DW factor,

also referred to as the non-ergodicity parameter [12], has been discussed by a number of

authors [12,13] and is of the form

$$D_w(q, T) = F_s(q, t_p) = \frac{1}{N} \left\langle \sum_j^N \exp(i\vec{q} \cdot \Delta\vec{r}_j(t_p)) \right\rangle \quad (5)$$

where F_s is the self intermediate scattering function and the time t_p is chosen to be

greater than the vibrational correlation time but less than the structural relaxation time

and so corresponds to the so-called plateau in the relaxation function. While different in

form to Eq. 4, Eq. 5 also defines the DW factor as the fraction of scattering associated

with elastic behavior, except now the separation between the two types of motion is made

using time rather than frequency.

The difference between the definitions of the DW factor for crystals and amorphous

solids is striking. The amorphous definition requires that the inelastic contribution is

measured and, in doing so, entangles the definition of the DW factor with the relaxation

dynamics. In contrast, the DW factor of the crystal is defined in terms of the elastic

scattering only and, as a result, is clearly identified as a purely structural measure. Can we obtain the amorphous DW factor using only elastic scattering data, just as in the crystal case? This capability would provide a number of significant benefits. First, it would allow us to use X-ray scattering, our main tool for structure determination in materials, to obtain DW factors. Secondly, it avoids the unnecessary need to resolve the frequency or time dependence of the scattering intensities. Finally, it would clarify the structural nature of the DW factor and, in so doing, support the interpretation of the DW factor as an order parameter for amorphous solidification. We shall now proceed to demonstrate that an analysis of the temperature dependence of elastic scattering from a coherent radiation source can indeed extract the DW factor for an amorphous material.

3. Amorphous Scattering from Incoherent and Coherent Sources

The total structure factor $S(\vec{q})$ is obtained from the measured scattering intensity $I(\vec{q})$ at the wavevector \vec{q} through the relation [14]

$$\begin{aligned}
 S(\vec{q}) &= 1 + \frac{I(\vec{q}) - \sum_{i=1}^N f_i^2(q)}{\frac{1}{N} \left[\sum_{i=1}^N f_i(q) \right]^2} \\
 &= 1 + \frac{\left\langle \sum_{j \neq k}^N f_j f_k \exp(-i\vec{q} \cdot (\vec{r}_j - \vec{r}_k)) \right\rangle_{\tau}}{\frac{1}{N} \left[\sum_{i=1}^N f_i(q) \right]^2}
 \end{aligned} \tag{6}$$

where f_j and \vec{r}_j are the form factor and position of atom j , N is the number of atoms and $\langle \dots \rangle_{\tau}$ is the average of the particle positions taken over some measurement time τ . In

selecting the measurement time τ one would ideally want the minimum value large enough to satisfy two requirements. The first is that enough photons are collected to provide an accurate determination of the scattering probability at each wavevector. The operational test for this condition is that there should be little variation in the measured intensity between two sequential measurements from a sample well below its glass transition temperature. The second requirement is that the measurement time be of sufficient duration to properly average over vibrational motion. In the case of computer simulations, we only need consider the second requirement since we calculate the scattering probability directly. In experiments, this situation is generally reversed. With Debye frequencies of the order of 10^{12} Hz, vibrational averaging is achieved within an extremely short time, no more than 10^{-6} s. Experimentally, the measurement time is entirely determined by the requirement to accumulate a sufficient number of photons per pixel to satisfy our operational test [15].

Eq. 6 assumes a coherent radiation source. Typical X-ray sources such as a rotating anode tube do not generate coherent radiation [16]. The resulting average over the phase variation of an incoherent source is equivalent to averaging over the intensities for different orientations of the wavevector \hat{q} , so that the structure factor $\bar{S}(q, T)$ reported for liquids and glasses is $\bar{S}(q, T) = \langle S(\vec{q}, T) \rangle_{\hat{q}}$ where $\langle \dots \rangle_{\hat{q}}$ is the average over the orientation of the wavevector at a fixed magnitude q and temperature T .

In this paper we have calculated $S(\vec{q}, T)$ for the binary $A_{80}B_{20}$ model glass former introduced by Kob and Anderson [17]. The molecular dynamics simulations are

performed at fixed NVT with the LAMMPS software [18], using a Nose-Hoover thermostat to keep the temperature constant. Our system consists of a binary mixture of 5,000 particles at a density of 1.20. All quantities are reported in reduced Lennard-Jones units as described in Ref [17]. The time step is set to 0.002 and a thermostat damping parameter of 0.2 is used. The simulations are initiated in relaxed glassy configurations generated using the Swap Monte Carlo algorithm at $T=0.05$ as described in Ref [3]. The energy of these configurations is then minimized using the LAMMPS implementation of the Polak-Ribiere conjugate gradient algorithm to give the $T=0$ structure. For each temperature considered, the system is initialized in the $T=0$ configuration, the thermostat is then set to the reported temperature, and the system is equilibrated for 10^6 timesteps before measurements are taken. Ten repeats of the simulation are performed starting from different initial configurations. The error bars correspond to the standard error, which are omitted when they are of comparable size to the symbol. The structure factor is calculated from the simulated configurations directly using Eq. 6. The measurement time is set to $\tau = 2 \times 10^4$, a value equal to the structural relaxation time τ_α at $T \sim 0.4$, and 1,000 configurations are evenly sampled over this time interval and used to compute the time average. In calculations of the scattered intensities we have set the form factors for species A and B to be equal.

In Fig. 1 the structure factor $\bar{S}(q, T)$ exhibits the modest dependence on T already well established in the literature [19]. ‘Modest’, we acknowledge, does not necessarily mean without interest. Mauro et al [20] reported a difference between the value of $\bar{S}(q_1, T)$ at the glass transition temperature and a value estimated by an extrapolation from higher T

that appears to correlate with the fragility. We do see, in Fig. 1b, evidence of a change in the temperature derivative of $\bar{S}(q_1, T) / \bar{S}(q_1, 0)$ similar to that seen experimentally [19,21].

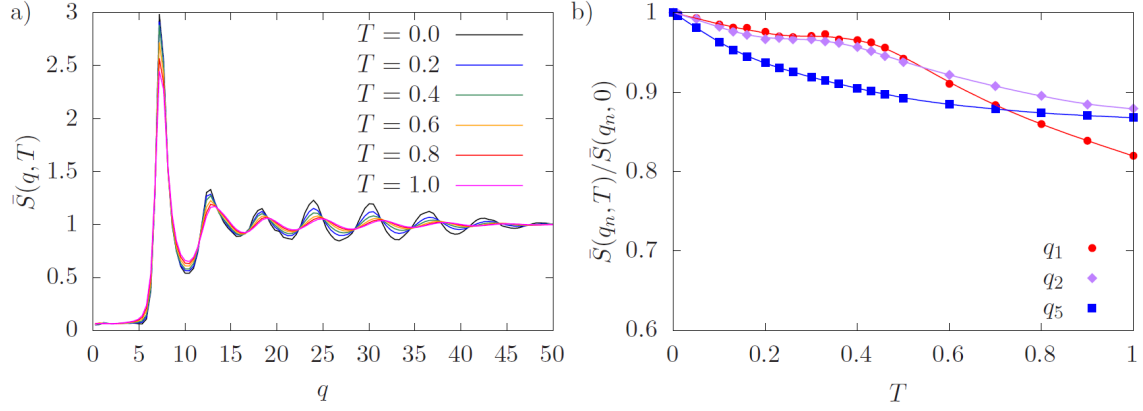


Figure 1. a) The dependence of the structure factor $\bar{S}(q, T)$ on the wavevector q for the simulated binary mixture for a range of temperatures. T and q are reported in reduced Lennard-Jones units as described in Ref. [17]. b) The temperature dependence of $\bar{S}(q_n, T) / \bar{S}(q_n, 0)$ (for $q_n = q_1, q_2$ and q_5 where q_n is the position of the n th peak in $\bar{S}(q, T)$).

Even though a transformation between fluid and solid has taken place over the temperature range studied, one accompanied by a large change in the amplitude of particle displacements, the weak temperature dependence of $\bar{S}(q, T)$ provides little indication of this. The culprit, it turns out, is the orientational averaging of the intensity. The angle-dependent scattering $S(\vec{q}, T)$ from an amorphous solid exhibits a complex granularity over the wavevector space referred to as *speckle* [22]. This speckle, as shown in Fig. 2, disappears on heating, leaving a uniform scattering intensity over of each

sphere in q -space characterized by a fixed wavevector magnitude q . The temperature dependence of this smoothing process is erased when we average over the wavevector orientation \hat{q} (or the phase of incoherent radiation). The problem we address in this paper is to extract a useful measure of structural restraint from the temperature dependence of $S(\vec{q}, T)$ *before* any averaging over wavevectors.

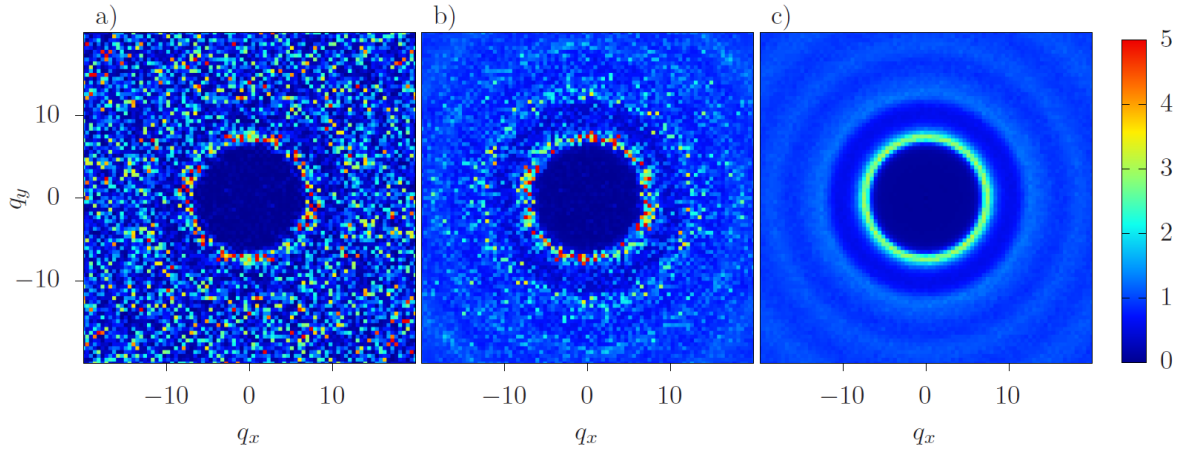


Figure 2. The scattering intensity $S(\vec{q})$, with intensities indicated by color as shown, in the (q_x, q_y) plane for a) $T = 0.0$ b) $T = 0.3$ and c) $T = 0.6$. The reduction of the intensity fluctuations (speckle) with increasing temperature is evident.

4. Analysis of the Temperature Dependence of the Speckle Scattering

We shall consider the explicit separation of the thermal fluctuations from the static disorder of the parent glass. Let $\vec{r}_j = \vec{R}_j + \vec{u}_j$ where \vec{R}_j is the position of the atom j in the parent $T=0$ configuration and \vec{u}_j its thermally excited displacement. Then

$$S(\vec{q}) = 1 + \frac{1}{N} \sum_{j \neq k} \exp[-i\vec{q} \cdot (\vec{R}_j - \vec{R}_k)] \left\langle \exp(-iP_{jk}(\vec{q})) \right\rangle_{\tau} \quad (7)$$

where $P_{jk}(\vec{q}) = \vec{q} \cdot (\vec{u}_j - \vec{u}_k)$. If the distribution of thermal displacements sampled during the measurement time τ can be treated as Gaussian, we can write

$$\left\langle \exp(-iP_{ij}(\vec{q})) \right\rangle_{\tau} = \exp(-\langle P_{ij}^2(\vec{q}) \rangle_{\tau} / 2) \quad (8)$$

Next, we shall separate this fluctuation term into its spatial mean and the local fluctuations about this mean, i.e.

$$\exp(-\langle P_{jk}^2(\vec{q}) \rangle_{\tau} / 2) = \langle \exp(-\langle P_{jk}^2(\vec{q}) \rangle_{\tau} / 2) \rangle_{jk} + h_{jk}(\vec{q}) \quad (9)$$

so that

$$S(\vec{q}, T) - 1 = \langle \exp(-\langle P_{jk}^2(\vec{q}) \rangle_{\tau} / 2) \rangle_{jk} [S(\vec{q}, 0) - 1] + \left(\frac{1}{N} \sum_{j \neq k} \exp(-\vec{q} \cdot \vec{R}_{jk}) h_{jk}(\vec{q}) \right) \quad (10)$$

This derivation has, so far, followed the standard treatment for the Debye-Waller factor for a crystal. The next step for the crystal would be to select only the wavevectors corresponding to peaks in intensity and determine the values of $S(\vec{q}, 0)$ from the analytic expressions for the perfect crystal. Amorphous scattering (like diffuse scattering from disordered crystals) distributes significant intensity across the continuum of \vec{q} space so that we need to generalize the analysis of the thermal contribution to disorder.

We propose the following. We shall partition phase space in terms of the magnitude of $S(\vec{q}, 0) - 1$ so that all of the values of \hat{q} (for a given magnitude q) for which $S(\vec{q}, 0) - 1$

lies within some narrow range about a selected value are grouped together. Then we can write

$$\langle S(\vec{q}, T) - 1 \rangle_{s_o} = \langle \langle \exp(-\langle P_{jk}^2(\vec{q}) \rangle_{\tau} / 2) \rangle_{jk} \rangle_{s_o} [S(\vec{q}, 0) - 1] + \left\langle \left(\frac{1}{N} \sum_{j \neq k} \exp(-\vec{q} \cdot \vec{R}_{jk}) h_{jk}(\vec{q}) \right) \right\rangle_{s_o} \quad (11)$$

where $\langle \dots \rangle_{s_o}$ indicates a restricted average of that set of wavevectors associated with a given value of $S(\vec{q}, 0) - 1$. Next, we shall assume that the two restricted averages on the RHS of Eq. 11 are independent of the value of $S(\vec{q}, 0) - 1$ so that we can rewrite Eq. 11 as

$$\langle S(\vec{q}, T) - 1 \rangle_{s_o} = D_w(q, T)[S(\vec{q}, 0) - 1] + H(q, T) \quad (12)$$

Eq.12 predicts a linear relation between the intensity at some non-zero T and the T=0 value with a slope and intercept that depend on T and q. As shown in Fig. 3, this prediction is empirically confirmed over a range of temperatures. This confirmation allows us to unambiguously extract the values of the $D_w(q, T)$ and $H(q, T)$ from scattering data and is the major result of this paper. $D_w(q, T)$ quantifies the residual correlation between the scattering at a non-zero T and T=0; so that $D_w = 1$ at T = 0 and goes to zero at the temperature at which the scattering is uniformly distributed (as shown in Fig. 2)

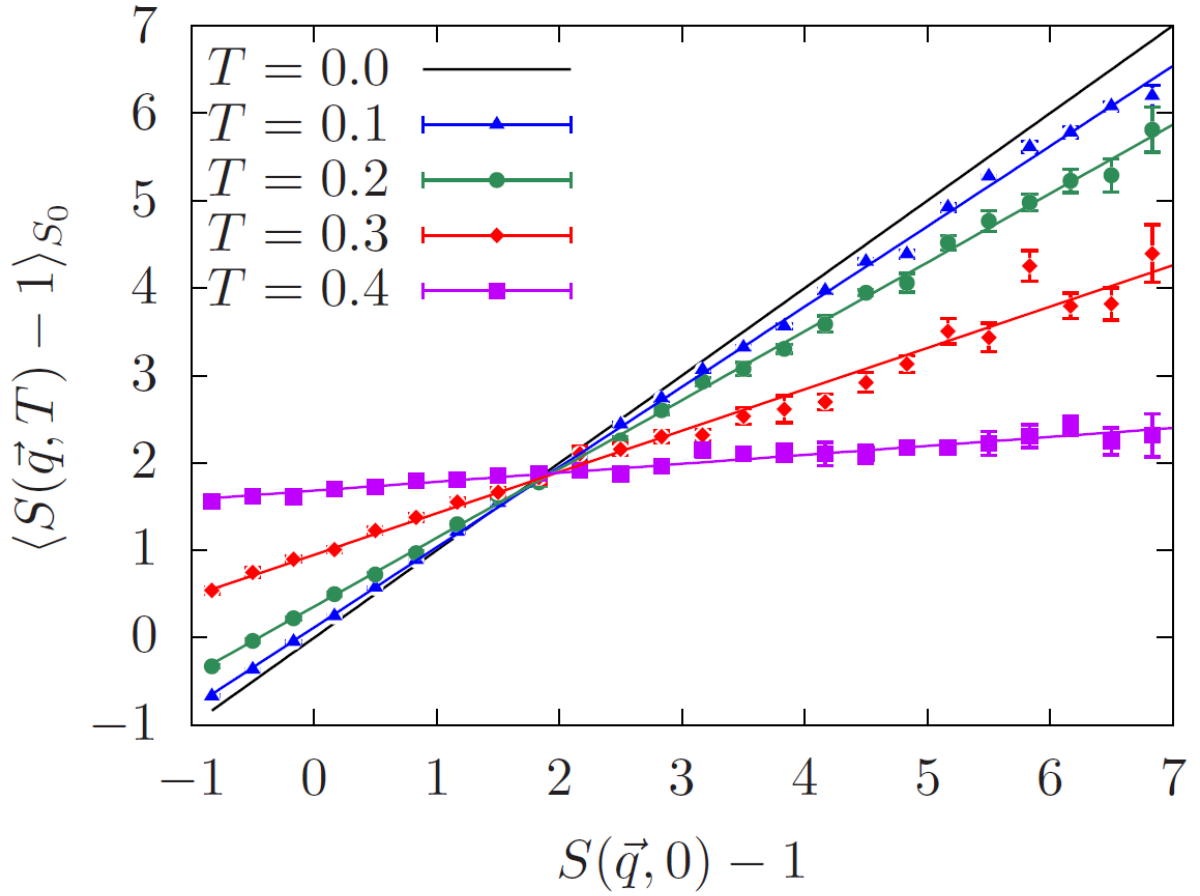


Figure 3. The variation of $\langle S(\vec{q}, T) \rangle_{S_0}$ with respect to the selected value of $S(\vec{q}, 0)$ (see text). Each color corresponds to a different temperature as indicated. The straight lines are least square fits.

The dramatic decrease of $D_w(q_1, T)$ from 1 to 0 on heating is in sharp contrast to the weak dependence of the structure factor itself, as shown in Fig. 4. As $D_w(q_1, T)$ is obtained from an analysis of the elastic scattering intensities, it represents a measure of structure that differentiates the liquid and the amorphous solid and, hence, satisfies the

requirements of an experimentally accessible structural order parameter for amorphous solidification. This was the goal of our study.

We can confirm that $D_w(q, T)$, as obtained from the linear fits in Fig. 3, is indeed the DW factor by comparing it to the theoretical value $D_o(q, T)$ based on a harmonic expansion [23],

$$D_o(q, T) \equiv \exp\left(-\frac{q^2}{3} \langle u_j^2 \rangle_\tau \right) \quad (13)$$

where we have neglected any correlation between the motions of different particles. As demonstrated in Fig. 4, $D_w(q_1, T) \approx D_o(q_1, T)$. Further confirmation of this connection is provided by the dependence of $\ln[D_w(q_1, T)]$ on q_1^2 (see Supplementary Material) where we find, at low T, the linear relation predicted by Eq. 13.

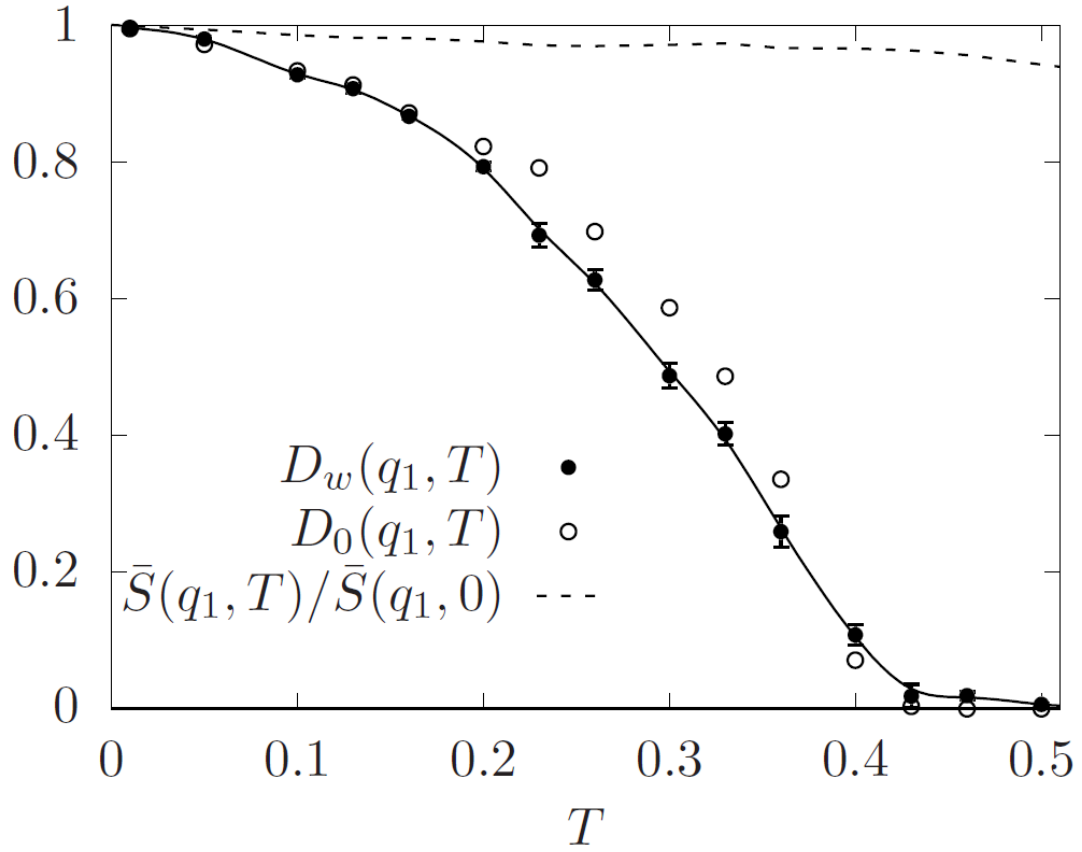


Figure 4. The temperature dependence of $D_w(q_1, T)$ and, for comparison, that of $\bar{S}(q_1, T)/\bar{S}(q_1, 0)$. Also plotted is $D_0(q_1, T)$ as defined in Eq.13. The curve is fitted to $D_w(q_1, T)$ as a guide to the eye.

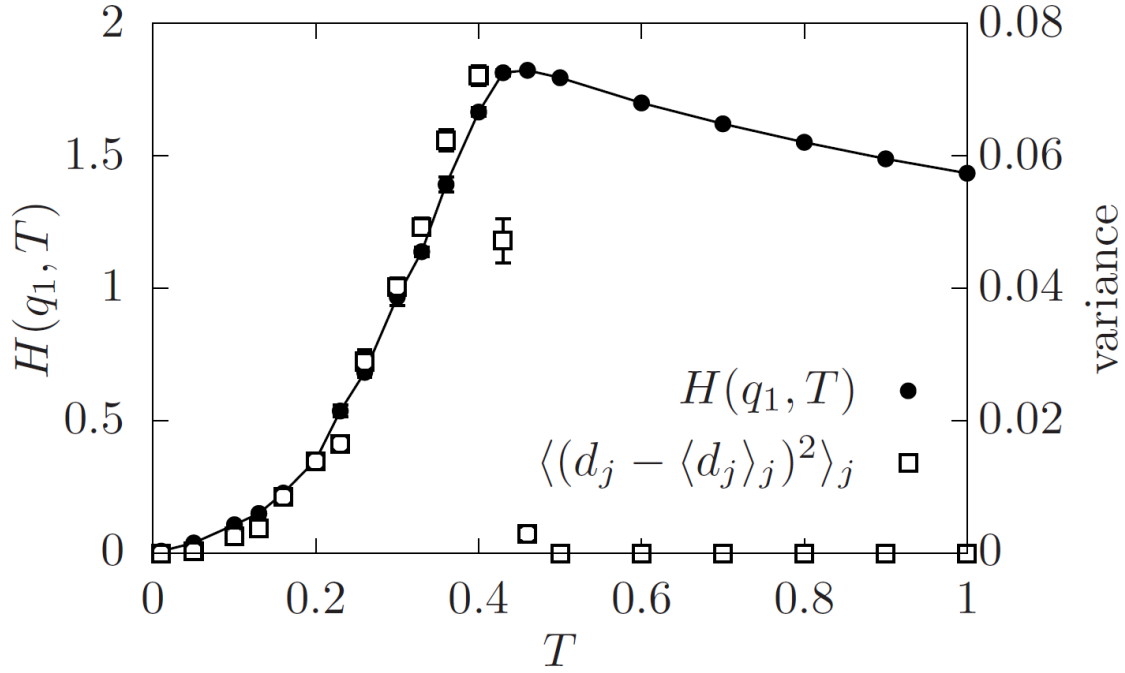


Figure 5. The quantity $H(q_1, T)$, obtained as the intercept from the analysis in Fig. 3, as

a function of T . Plotted on the right axis is the variance $\langle (d_j - \langle d_j \rangle_j)^2 \rangle_j$ where

$$d_j = \exp\left(-\frac{q_1^2}{3} \langle u_j^2 \rangle_\tau\right). \text{ The curve is fitted to } H(q_1, T) \text{ as a guide to the eye.}$$

The plot in Fig. 3 also allows us to extract $H(q_1, T)$ from the intercept, which we have plotted against temperature in Fig. 5. As indicated in the derivation of Eq. 11, $H(q_1, T)$ is associated with the spatial variation in the amplitude of the thermal fluctuations in atomic positions. To confirm this connection, we have calculated the spatial variance in the

quantity $d_j = \exp\left(-\frac{q_1^2}{3} \langle u_j^2 \rangle_\tau\right)$ and plotted the results in Fig. 5. Apart from a scaling constant, the variance closely matches the values of $H(q_1, T)$ up to value of T at which the variance abruptly vanishes. The dramatic rise and fall in $\left\langle (d_j - \langle d_j \rangle)^2 \right\rangle_j$ reflects the twin effects of increasing temperature: enhanced fluctuations and increased relaxation rate. The former produces the increase in the variance, observed at low T, while the increasing rate of relaxation ends up smoothing out fluctuations (as shown in Fig. 2). The competing effects of increased amplitude of thermal fluctuations and increased relaxation rate of these fluctuations with increasing T results in a crossover in $H(q_1, T)$; at lower values of T, H provides a measure of the variance of the structural restraint while above this crossover temperature $H(q_1, T) = \bar{S}(q_1, T)$, the structure factor. The existence of the maximum appears to be universal, but its exact position is dependent on the choice of measurement time (see Supplementary Materials). These results establish that our analysis of the speckle intensities can not only extract information about the mean value of the atomic restraint but information about its spatial heterogeneity, in the form of the variance, as well. This is an exciting result as there is a growing theoretical consensus [24-27] that the mechanical properties of glasses are best understood as a consequence of a spatial distribution of rigidity. On the length scales of individual atoms, this mechanical heterogeneity is manifest as a distribution of atomic restraint [28] which we have demonstrated can be measured (to within a temperature independent constant).

5. Conclusions

In conclusion, we have established that it is possible to directly measure a dramatic change in the structure of an amorphous material during changes in temperature from an analysis of the elastic scattering from the material using a coherent radiation source. This structural change is in the form of the amorphous Debye-Waller factor $D_w(q_1, T)$ and corresponds to an experimental measure of the degree of restraint imparted by a configuration over the measurement time. The DW factor that we have extracted from the elastic scattering is quantitatively similar to the value obtained from the previous definition based on the analysis of inelastic scattering (see Supplementary Material). The quantity $D_w(q_1, T)$ meets the two essential prerequisites of a structural order parameter: a) it is obtained by a structural measurement, static scattering in this case, and b) it is capable of differentiating the amorphous solid from the liquid, as demonstrated in Fig.4. Previously [2,3], we have argued that structural restraint provides a much more useful characterization of amorphous structure than more traditional measures based on topology or geometry. The analysis presented in this paper also provides a second quantity, $H(q_1, T)$, that we have shown is proportional to the variance of the local restraint below some threshold temperature. This quantity provides a direct experimental measure of the amplitude of spatial heterogeneity of structural restraint in an amorphous material.

The ultimate object of this study is to establish how to extract useful information from real experimental measurements of speckle intensity in glass forming materials. How feasible are such experiments? Speckle intensities are routinely resolved and measured

using X-ray photon correlation spectroscopy for metallic [29], oxide [30] and colloidal glasses [31] over a wide range of temperatures. These experiments make use of coherent X-rays generated at synchrotron facilities. As the measurements proposed here require exactly the same measured intensities, there appears to be no significant obstacle to experimentally test for the linearity reported in Fig. 3 and the extraction of the Debye-Waller factor $D_w(q_1, T)$ and the associated quantity $H(q_1, T)$.

If confirmed experimentally, these results would establish that the structural transformation, amorphous solidification, can be monitored directly through the analysis of the static speckle scattering. With this new capability comes the opportunity to rethink the very framework of glassy phenomenology; to explore how the temperature dependence of fundamental features of amorphous materials, such as fragility, elastic response, yield stress and thermal conductivity, are related directly to the measured change in structure.

Acknowledgements

CFP and PH gratefully acknowledge Gang Sun for providing equilibrated initial atomic configurations and helpful discussions with Amelia Liu and Tim Petersen. CFP is the recipient of an Australian Research Council Discovery Early Career Award (DE210100256) funded by the Australian Government. This research was undertaken with the assistance of resources and services from the National Computational Infrastructure (NCI), which is supported by the Australian Government.

References

1. Definition of the glass transition from IUPAC, *Compendium of Chemical Terminology*, 2nd Ed. (1997).
2. G. Sun, L. Li and P. Harrowell, The structural difference between strong and fragile liquids. *J. Non-Cryst. Sol.* **13**, 100080 (2022).
3. G. Sun and P. Harrowell, A general structural order parameter for the amorphous solidification of a supercooled liquid. *J. Chem. Phys.* **157**, 024501 (2022).
4. G. Sun and P. Harrowell, Amorphous solidification of a supercooled liquid in the limit of rapid cooling. *J. Chem. Phys.* **158**, 204506 (2023)
5. G. Sun, S. Saw, I. Douglass and P. Harrowell, Structural origin of enhanced dynamics at the surface of a glassy alloy. *Phys. Rev. Lett.* **119**, 245501 (2017).
6. P. Debye, *Annalen der Phys.* **348**, 49-92 (1913).
7. J. Als-Nielsen and D. McMorrow, *Elements of Modern X-ray Physics*. (John Wiley, Nw York, 2011).
8. D. W. J. Cruickshank, The determination of the anisotropic thermal motion of atoms in crystals. *Acta Cryst.* **9**, 747 (1956).
9. *The Rietveld Method*, ed. R. A. Young (Oxford University Press, London, 1993).

10. B. Frick, D. Richter, W. Petry and U. Buchenau, Study of the glass transition order parameter in amorphous polybutadiene by incoherent neutron scattering. *Z. Phys. B-Cond. Matt.* **79**, 73-79 (1988).
11. U. Buchenau and R. Zorn, A relation between fast and slow motions in glassy and liquid Selenium. *EPL* **18**, 523 (1992).
12. F. Sciortino and W. Kob, The Debye-Waller factor of liquid silica: Theory and simulation. *Phys. Rev. Lett.* **86**, 648-651 (2001).
13. S. Jabbari-Farouji, H. Tanaka, G. H. Wegdam and D. Bonn, Multiple nonergodic disordered state in Laponite suspensions: A phase diagram. *Phys. Rev. E* **78** 061405 (2008).
14. N. A. Mauro, A. J. Vogt, M. L. Johnson, J. C. Bendert, R. Soklaski, L. Yang and K. F. Kelton, Anomalous structural evolution and liquid fragility signatures in Cu-Zr and Cu-Hf liquids and glasses, *Acta Mater.* **61**, 7411-7421 (2013).
15. B. E. Warren, *X-ray Diffraction* (Dover, London, 1969).
16. N. A. Dyson. *X-Rays in Atomic and Nuclear Physics* (2nd Edition) (Cambridge UP, Cambridge, 1990).
17. W. Kob and H. C. Andersen, Testing mode-coupling theory for a supercooled binary Lennard-Jones mixture I: The van Hove correlation function. *Phys. Rev. E* **51**, 4626-4641 (1995).

18. A. P. Thompson et al., LAMMPS - a flexible simulation tool for particle-based materials modeling at the atomic, meso, and continuum scales, *Comp Phys Comm*, **271**, 10817 (2022).
19. E. Bartsch, H. Bertagnolli, P. Chieux, A. David and H. Sillescu, Temperature dependence of the static structure factor of ortho-terphenyl in the supercooled liquid regime close to the glass transition. *Chem. Phys.* **169**, 373-378 (1993).
20. N. A. Mauro, M. Blodgett, M. L. Johnson, A. J. Vogt and K. F. Kelton, A structural signature of liquid fragility. *Nature Com.* **10**, 1038 (2014).
21. C. W. Ryu, W. Dmowski, K. F. Kelton, G. W. Lee, E. S. Park, J. R. Morris and T. Egami, Curie-Weiss behavior of liquid structure and ideal glass state. *Sci. Rep.* **9**, 18579 (2018).
22. J. W. Goodman, Some fundamental properties of speckle. *J. Opt. Soc. Am.* **66**, 1145-1150 (1976).
23. L. V. Meisel and P. J. Cote, Structure factors in amorphous and disordered harmonic Debye solids. *Phys. Rev. B* **16**, 2978-2980 (1977).
24. M. Tsamados, A. Tanguy, C. Goldenberg and J.-L. Barrat, Local elasticity map and plasticity in a model Lennard-Jones glass. *Phys. Rev. E* **80**, 026112 (2009).
25. H. Wagner, D. Berdorf, S. Kuchemann, M. Schwabe, B. Zhang, W. Arnold and K. Samwer, Local elastic properties of a metallic glass. *Nature Mat.* **10**, 439-442 (2011).

26. G. Kapteijns, D. Richard, E. Bouchbinder and E. Lerner, Elastic moduli fluctuations predict wave attenuation rate in glasses. *J. Chem. Phys.* **154**, 081101 (2021).
27. M. Lerbinger, A. Barbot, D. Vandembroucq and S. Patinet, Relevance of shear transformations in the relaxation of supercooled liquids. *Phys. Rev. Lett.* **129**, 195501 (2022).
28. S. Saw and P. Harrowell, Rigidity in condensed matter and its origin in configurational constraint. *Phys. Rev. Lett.* **116**, 137801 (2016).
29. N. Neuber, et al, Disentangling structural and kinetic components of the α -relaxation in supercooled metallic liquids, *Comm. Phys.* **5**, 316 (2022).
30. E. Alfinelli, F. Caporaletti, F. Dallari, A. Martinelli, G. Monaco, B. Ruta, M. Sprung, M. Zanatta and G. Baldi, Amorphous-amorphous transformation induced in glasses by intense x-ray beams. *Phys. Rev. B* **107**, 054202 (2023)
31. F. A. de Melo Marques, R. Angelini, E. Zaccarelli, B. Farago, B. Ruta, G. Ruocco and B. Ruzicka, Structural and microscopic relaxations in a colloid glass. *Soft Matter* **11**, 466 (2015).

SUPPLEMENTARY MATERIAL

Direct Measurement of the Structural Change Associated with Amorphous Solidification using Elastic Scattering of Coherent Radiation

Charlotte F. Petersen^{1,2} and Peter Harrowell^{1,*}

¹*School of Chemistry, University of Sydney, Sydney, New South Wales 2006 Australia*

²*School of Chemistry, University of Melbourne, Melbourne, Victoria 3010 Australia*

* Corresponding author: peter.harrowell@sydney.edu.au

Contents

1. *The q Dependence of $D_w(q, T)$*
2. *The Comparison of the Debye-Waller factor from Elastic Scattering and that based on the Self-Intermediate Scattering Function $F_s(q, t)$*
3. *The Dependence of $H(q, T)$ on the Measurement Time τ*

1. The q Dependence of $D(q, T)$

A characteristic of the Gaussian assumption used to derive the Debye-Waller factor, in general, and, specifically, in Eq. 13 is a dependence on q that goes as $\ln D_o(q, T) \propto q^2$. We can check to see whether $D_w(q, T)$ also exhibits this same dependence. In Fig. S1 we have plotted $\ln D_w(q, T)$ against q^2 and find the predicted linear relationship at low T , providing an additional support for our identification of $D_w(q, T)$ as the Debye-Waller factor. At higher temperatures, we do see signs of a deviation from this behaviour where the slope in Fig. S1 decreases with increasing q .

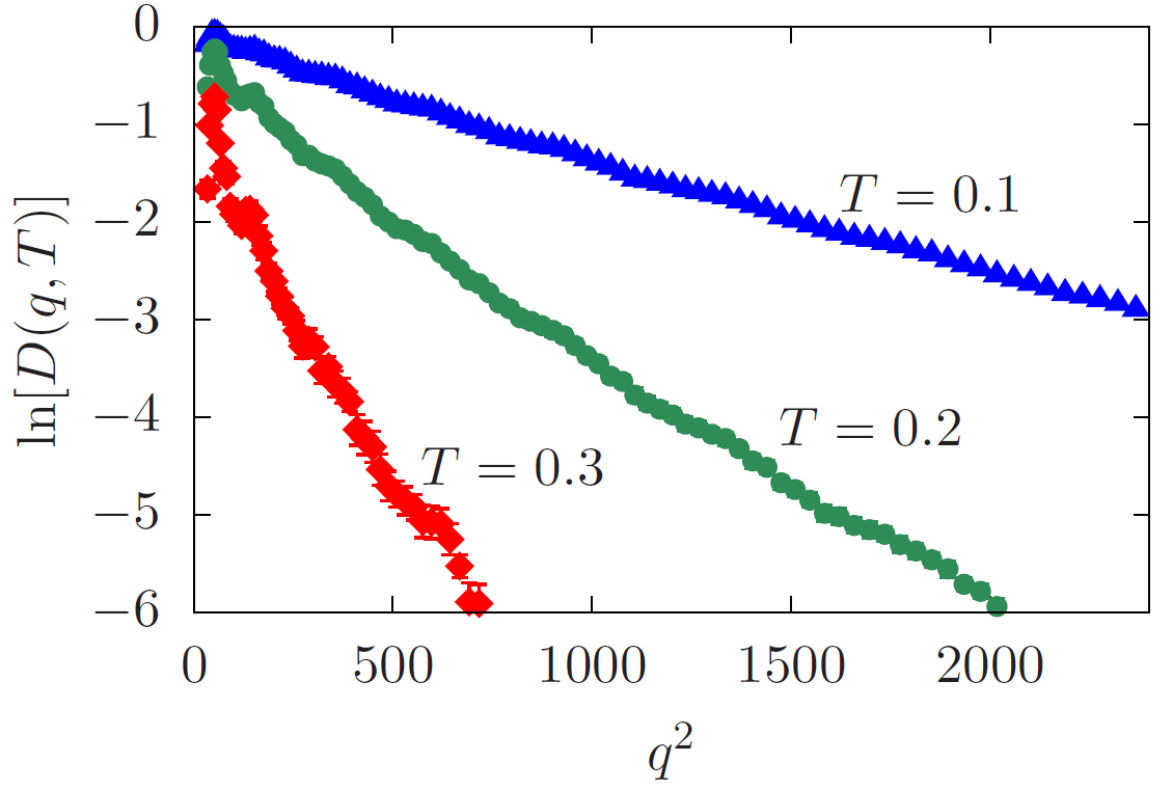


Figure S1. The dependence of $\ln D_w(q, T)$ on q^2 for three temperatures as indicated.

2. The Comparison of the Debye-Waller factor from Elastic Scattering and that based on the Self-Intermediate Scattering Function $F_s(q, t)$

The self-intermediate scattering function $F_s(q, t)$ is calculated using

$$F_s(q, t) = \frac{1}{N} \left\langle \sum_j^N \exp(i\vec{q} \cdot \Delta\vec{r}_j(t)) \right\rangle \quad (\text{S2})$$

where $\Delta\vec{r}_j(t) = \vec{r}_j(t) - \vec{r}_j(0)$ and the average is taken over different initial configurations and different orientations of the wavevector \vec{q} and plotted against $\log(t)$ in Fig. S2. An estimate of the Debye-Waller factor has been proposed [12,13], equal to the plateau height of $F_s(q, t)$. We shall define the plateau height by the measurement time $\tau = 2 \times 10^4$ used in this present paper as indicated in Fig. S2.

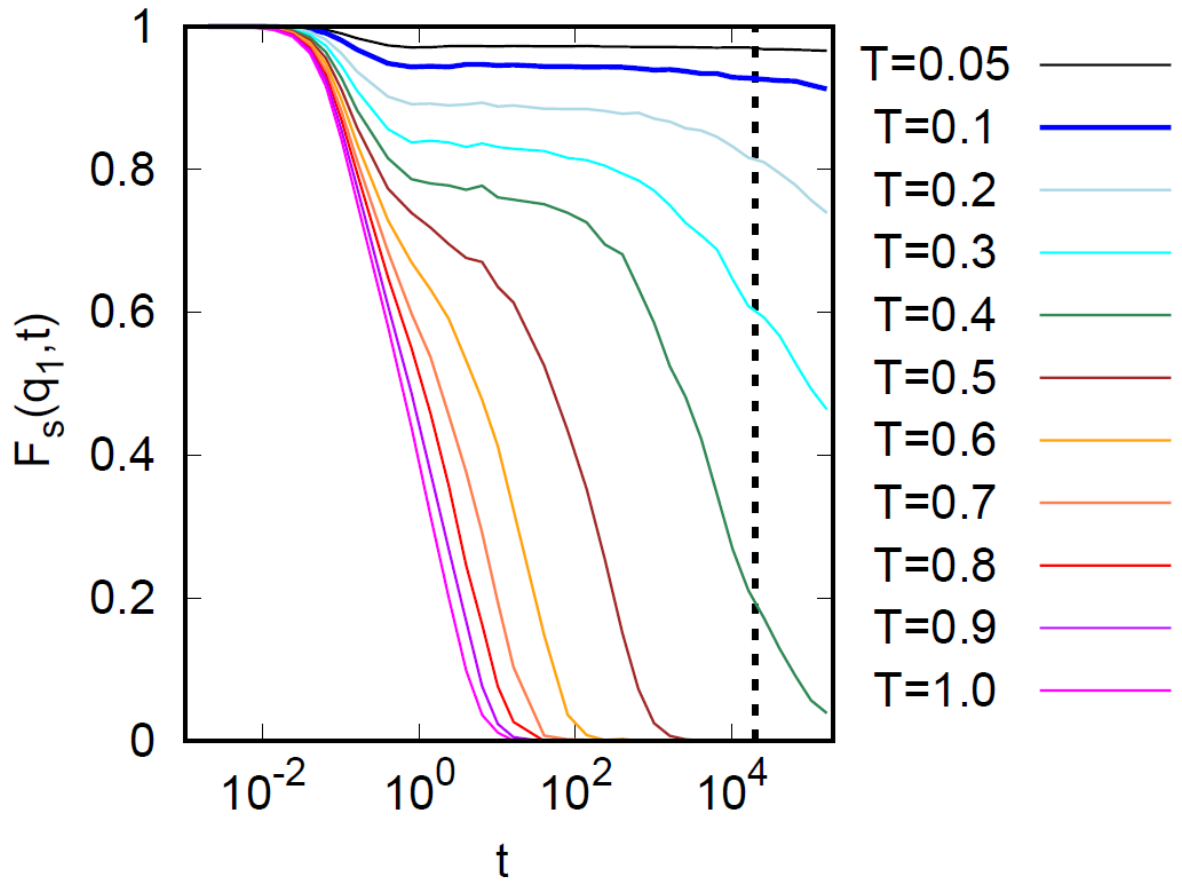


Figure S2. The self-intermediate scattering function $F_s(q, t)$ calculated at $q = q_1$ for a range of temperatures as indicated. The measurement time τ is indicated by the vertical dashed line.

In Fig. S3 we compare $D_o(q_1, T)$ with the DW factor $D_w(q_1, T)$ extracted from the scattering intensities and the quantity $D_o(q_1, T)$ obtained from the calculated mean squared displacements using the harmonic approximation. We find excellent agreement between $F_s(q, \tau)$ and $D_o(q_1, T)$. While there is some deviation between $D_o(q_1, T)$ and $D_w(q_1, T)$ at intermediate temperatures, there is strong agreement between the two quantities at both low T and the higher temperature at which both quantities vanish.

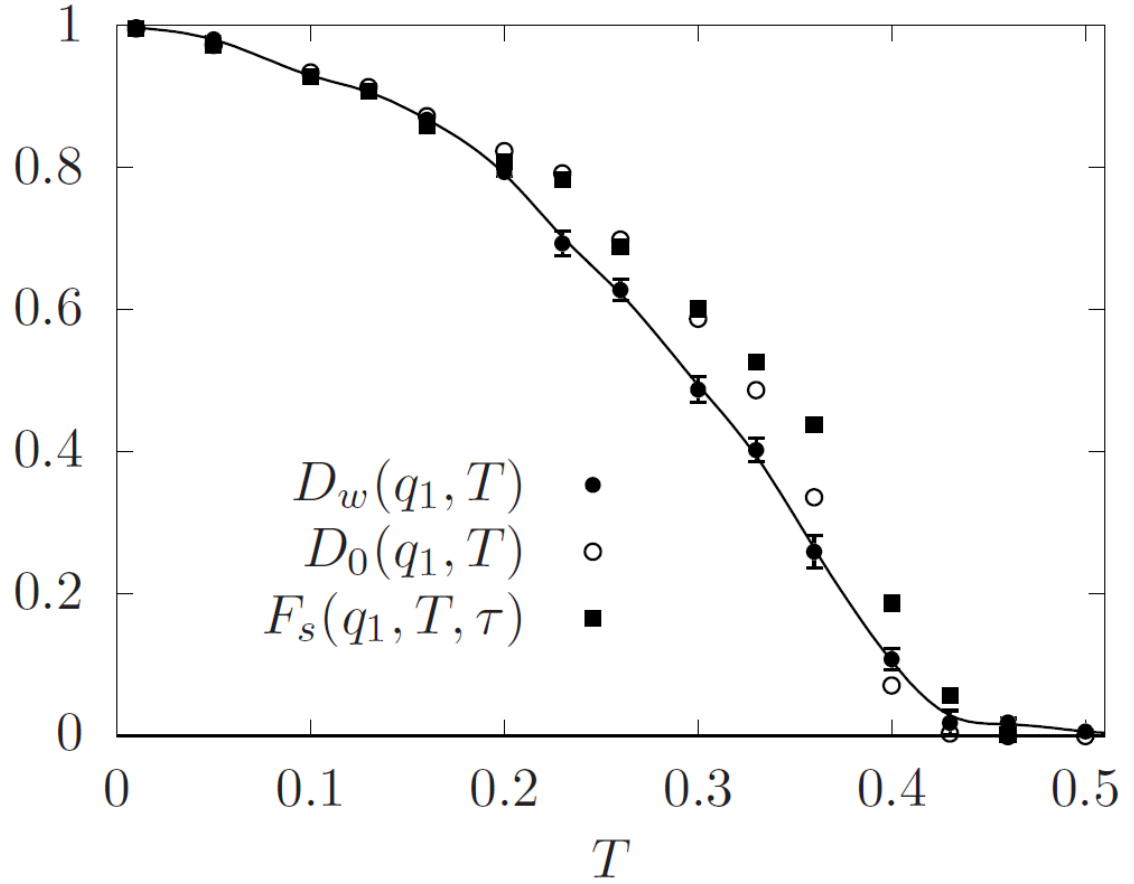


Figure S3. A comparison of the Debye-Waller factor $D_w(q_1, T)$ calculated from the elastic scattering and the harmonic approximation $D_0(q_1, T)$ with the estimate equal to $F_s(q_1, T, \tau)$. The time τ is the same measurement time as used in calculating $D_w(q_1, T)$.

3. The Dependence of $H(q, T)$ on the Measurement Time τ

In Fig. S4 we compare the temperature dependence of the quantity $H(q_1, T)$ and the variance of the local restraint $d_j = \exp\left(-\frac{q_1^2}{3} \langle u_j^2 \rangle_\tau\right)$ calculated using two different values of the measurement time, i.e. $\tau = 2 \times 10^4$ and 2×10^6 . We find that the general shape of the curves including the cusps in both quantities are unaltered in form but that both maxima shift to a slightly lower temperature with the longer measurement time interval.

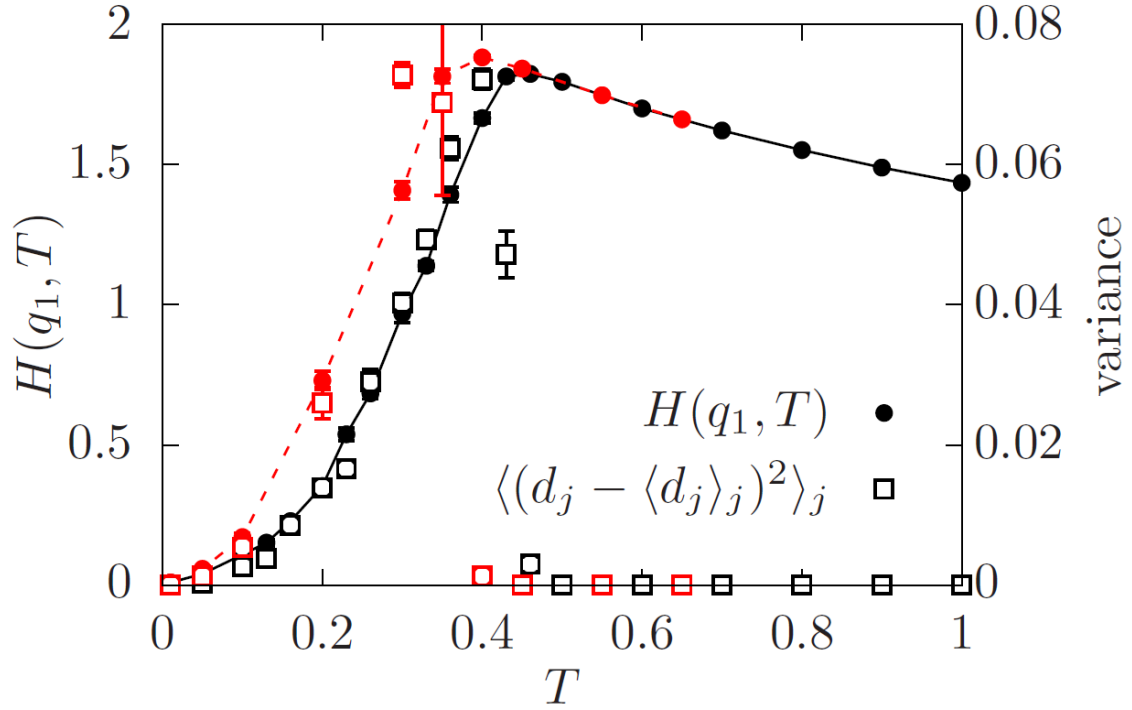


Figure S4. The quantity $H(q_1, T)$, obtained as the slope from the analysis in Fig. 3, as a function of T . Plotted on the right axis is the variance $\langle (d_j - \langle d_j \rangle_j)^2 \rangle_j$ where

$$d_j = \exp\left(-\frac{q_1^2}{3} \langle u_j^2 \rangle_\tau\right).$$

Two different values of the measurement time have been used: $\tau = 2 \times 10^4$ (black symbols) and 2×10^6 (red symbols). The curve is fitted to $H(q_1, T)$ as a guide to the eye.